J. Vis. Commun. Image R. 24 (2013) 867–884

Contents lists available at SciVerse ScienceDirect

J. Vis. Commun. Image R.

journal homepage: www.elsevier.com/locate/jvci

Universal intra coding for arbitrary RGB color filter arrays in HEVC

Yung-Hsiang Chiu [a], Kuo-Liang Chung [a], Wei-Ning Yang [b], Chien-Hsiung Lin [a,*], Yong-Huai Huang [c]

[a] Department of Computer Science and Information Engineering, National Taiwan University of Science and Technology, No. 43, Section 4, Keelung Road, Taipei 10672, Taiwan, ROC
[b] Department of Information Management, National Taiwan University of Science and Technology, No. 43, Section 4, Keelung Road, Taipei 10672, Taiwan, ROC
[c] Institute of Computer and Communication Engineering, Department of Electronic Engineering, Jinwen University of Science and Technology, No. 99, AnChung Road, Hsin-Tien, New Taipei City 23154, Taiwan, ROC

ARTICLE INFO

Article history:
Received 1 March 2013
Accepted 25 May 2013
Available online 12 June 2013

Keywords:
Arbitrary color filter arrays
BD-BR
BD-PSNR
Bitrate
Demosaicing
H.264/AVC
HEVC
Mosaic video sequences
PSNR
Universal intra coding

ABSTRACT

Compressing mosaic video sequences is necessary for storage and transmission over the internet. However, mosaic video sequences with different red–green–blue (RGB) color filter arrays (CFAs) require different compression schemes. We propose a two-stage universal intra coding scheme for compressing mosaic video sequences with arbitrary RGB-CFAs in high efficiency video coding (HEVC). Based on the associated mosaic structure, the proposed scheme first demosaics the neighboring reference pixels and then predicts the color value of the target pixel using the color values of the identical color components in the demosaiced reference pixels. Experimental results demonstrate that the proposed universal intra coding scheme achieves substantial improvement on bitrate while preserving the quality of the reconstructed video sequences.

1. Introduction

With the advance in multimedia technology, digital cameras become increasingly ubiquitous. For the consideration of cost, most consumer digital cameras are equipped with a light sensor and a red–green–blue (RGB) color filter array (CFA) structure to capture color information [18]. The structures of color filters in the RGB-CFA are usually designed by the camera manufacturers and referred to as the mosaic structures. Ten commonly used types of the RGB-CFAs [16] are shown in Fig. 1 and the Bayer CFA [1] is the most well-known structure among them. The camera with specific RGB-CFA structure produces mosaic video sequences by selecting only one of the RGB color components for each pixel in the image frame. To reconstruct a full color video sequence, the missing color components of each pixel in the image frame are estimated by the demosaicing process, which has been extensively studied in [5,6,10,13–17,19,20,22–24].

In addition to the demosaicing process, another important issue for mosaic video sequences is video compression, which is necessary for storage saving and transmission over the internet. Compression schemes for mosaic video sequences can be divided into two categories: structure conversion based and color recovering based schemes. The former converts the CFA structure into three distinct color planes for compression and the latter recovers the full RGB colors for compression. Structure conversion based compression schemes are often applied to compress mosaic video sequences with the Bayer CFA structure since the Bayer CFA is easier to convert than other CFA structures and has 2:1:1 (G:B:R) color component composition which is similar to the 4:2:2 sampling format for the encoder. Gastaldi et al. [9] presented the first mosaic video coders for compressing the sequences with the Bayer CFA under the MPEG-2 environment [26], where each mosaic image frame is decomposed into three distinct rectangular color planes which are individually compressed to increase the compression ratio. Since H.264/AVC video coders [25] usually achieves better compression performance than MPEG-2 video coders, Doutre et al. [7] incorporated the structure conversion technique in [12] with the prediction schemes in H.264/AVC to tackle the mosaic video sequences with the Bayer CFA structure. Doutre and Nasiopoulos [8] further modified, according to the Bayer CFA structure, the intra prediction scheme in H.264/AVC to enhance the quality of the reconstructed video sequence. However, due to the requirement of specific sampling format by an encoder and the difficulty in converting irregular CFA patterns, the structure conversion based compression schemes cannot be used directly to compress mosaic video sequences with non-Bayer CFAs.

* Corresponding author.
E-mail address: d9409301@mail.ntust.edu.tw (C.-H. Lin).

1047-3203/$ - see front matter © 2013 Elsevier Inc. All rights reserved.
http://dx.doi.org/10.1016/j.jvcir.2013.05.012

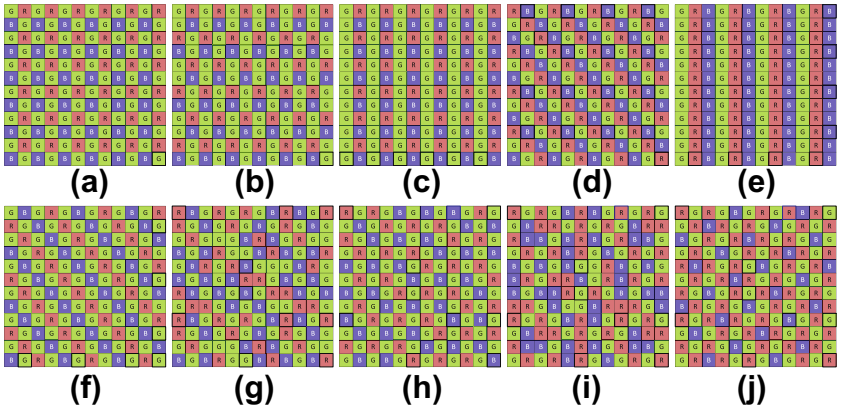

Fig. 1. Ten typical RGB-CFAs: (a) Bayer CFA, (b) Lukac and Plataniotis CFA, (c) Yamanaka CFA, (d) diagonal stripe CFA, (e) vertical stripe CFA, (f) modified Bayer CFA, (g) HVS-based CFA, (h) type I pseudo-random CFA, (i) type II pseudo-random CFA and (j) type III pseudo-random CFA.

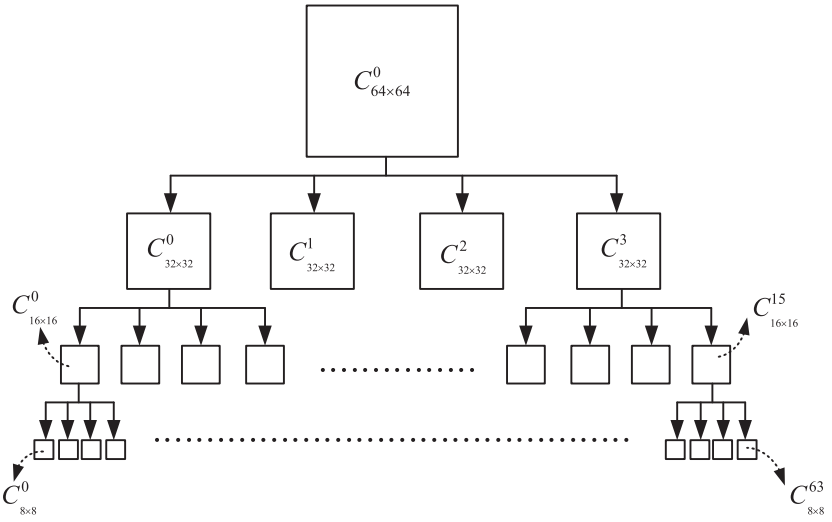

Fig. 2. The quadtree structure for coding units.

Instead of converting the structure, demosaicing the mosaic video sequence prior to compressing is another approach. Prior to compression, Chen et al. [4] first recovered the full RGB colors for a mosaic video sequence with the Bayer CFA structure and then adjusted the chroma subsampling strategy in H.264/AVC to improve the quality of the reconstructed mosaic video sequences. Yang et al. [21] proposed a universal compression scheme for mosaic video sequences with arbitrary RGB-CFAs in H.264/AVC, which, prior to compression, basically combines and modifies the universal demosaicing method by Lukac and Plataniotis [15] and the subsampling method by Chen et al. [4]. The color recovering based compression schemes avoid the difficulty of structure conversion but suffer from the color deviations from color domain transformation [27]. Consequently, the reconstructed video sequence using color recovering based compression schemes may have poor compression performance.

As the resolution of video sequences increases, the H.264/AVC standard can no longer deliver satisfied compression results. A high efficiency video coding [3], abbreviated as HEVC, is developed to improve the compression efficiency for high resolution video sequences. When compressing mosaic video sequences using the HEVC standard, one natural approach is to adapt the compression schemes in H.264/AVC to the HEVC standard. However, the structure conversion based compression schemes cannot be applied in HEVC since the sampling format required for structure conversion is not supported in HEVC and the color recovering compression schemes still suffer from problem caused by color domain transformation in HEVC. Thus, developing a universal compression scheme in HEVC for mosaic video sequences with arbitrary RGB-CFAs is important, leading to main motivation of this research.

In this paper, we propose a two-stage universal intra coding scheme in HEVC for compressing mosaic video sequences with arbitrary RGB-CFAs. In the first stage, the proposed scheme demosaics, according to the associated mosaic structure, the pixels in the reference row and column. Based on the associated mosaic structure, the second stage predicts the color value for a mosaiced pixel with a specific color component using the demosaiced reference pixels with the identical color component. The proposed scheme is universal since no structure conversion is involved and a demosaicing scheme for arbitrary CFA structure is available. Furthermore, the proposed scheme avoids the quality degradation in the reconstructed video sequences since no color domain transformation is required. Experimental results on ten typical RGB-CFAs demonstrate that the proposed universal intra coding scheme can achieve substantial bitrate reduction and quality improvement over the existing intra coding schemes. To the best of our knowledge, the proposed scheme is the first universal intra coding scheme designed specifically for mosaic video sequences with arbitrary RGB-CFAs in HEVC.

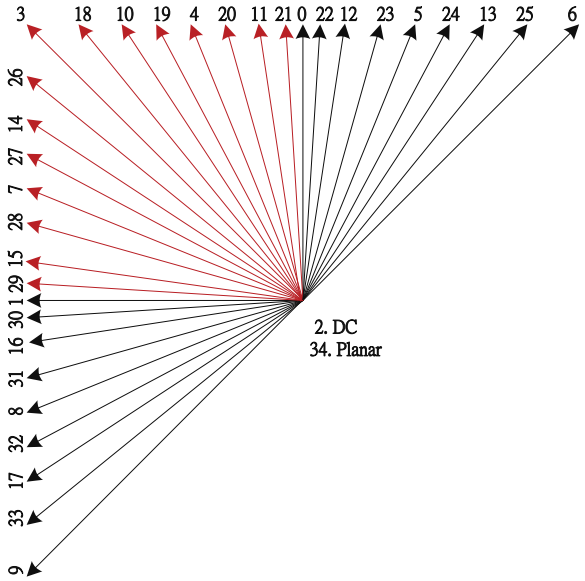

Fig. 3. Available 35 intra prediction modes in HEVC.

The rest of this paper is organized as follows. Section 2 introduces the conventional intra coding scheme in HEVC. In Section 3, we present the proposed universal intra coding scheme for the mosaic video sequences with arbitrary RGB-CFAs in HEVC. Section 4 gives, based on the video sequences with ten typical RGB-CFAs, the empirical results on the compression performance of the quality of the reconstructed video sequence and the bitrate. Concluding remarks are given in Section 5.

2. Intra coding scheme in HEVC

In this section, we introduce the intra coding scheme in HEVC. The notations defined in this section will be used in the next section for describing the proposed universal intra coding scheme in HEVC. When compressing the video sequences by the HEVC encoder, coding unit is the basic unit to be encoded for each image frame. Each image frame in a video sequence is first partitioned into a set of non-overlapping 64×64 coding units, each of which is further partitioned down to 8×8 coding units. The partitions of a 64×64 coding unit are usually modeled by a recursive quadtree decomposition and can be represented as a hierarchical structure of coding units, as shown in Fig. 2, where $C^0_{N\times N}, C^1_{N\times N}, \ldots, C^{(64/N)^2-1}_{N\times N}$ denote the $(64/N)^2$ coding units of size $N \times N$ for $N = 64, 32, 16, 8$.

Each coding unit in the quadtree is encoded by either intra prediction scheme or inter prediction scheme. Exploiting the spatial redundancy existing in each image frame, the intra prediction scheme predicts the luma and chroma values of each pixel in the current coding unit by referring to the neighboring encoded pixels. Exploiting the temporal redundancy existing in consecutive frames, the inter prediction scheme predicts the luma and chroma values of each pixel in the current coding unit by referring to the previous frames. Different prediction schemes may result in different storage requirement and quality for the current coding unit. The rate-distortion (RD) cost which considers the tradeoff between the bitrate and the distortion is the criterion for determining the prediction scheme for each coding unit. The prediction scheme that results in the minimum RD cost is adopted for the current coding unit.

In intra prediction, for each coding unit of size $N \times N$ with $N = 64, 32, 16$, there is only one prediction unit of size $N \times N$, whereas for coding unit of size 8×8, there exist two kinds of prediction units of sizes 8×8 and 4×4. For $N = 64, 32, 16$, let $P^{i,0}_{N\times N}$ denote the prediction unit corresponding to the coding unit $C^i_{N\times N}$ for $i = 0, 1, \ldots, (64/N)^2 - 1$. Denote by $P^{i,0}_{8\times 8}$ the prediction unit of size 8×8 and $P^{i,j}_{4\times 4}$ with $j = 0, 1, 2, 3$ the four prediction units of size 4×4 corresponding to the coding unit $C^i_{8\times 8}$.

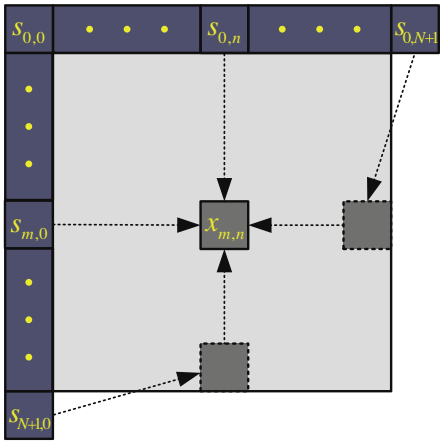

Fig. 5. Planar intra prediction mode in HEVC.

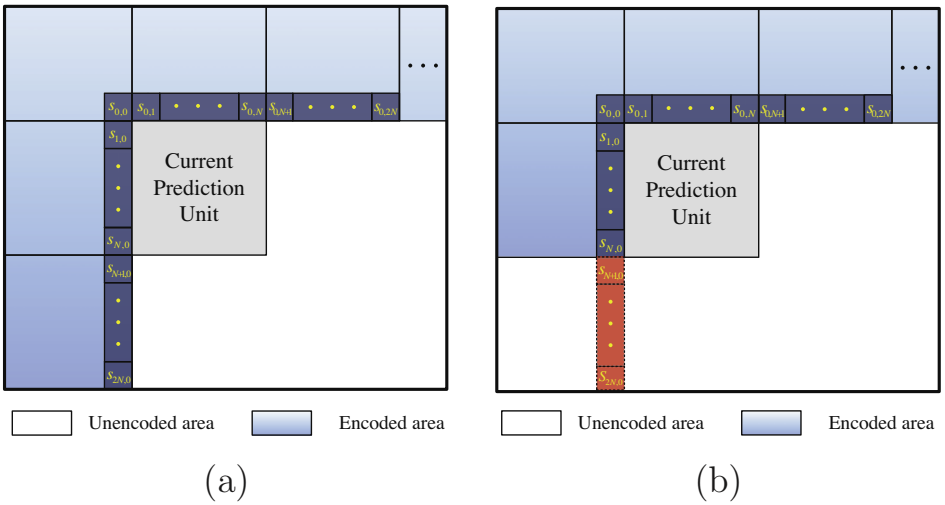

Fig. 4. Reference pixels for intra prediction in HEVC. (a) All reference pixels are available and (b) reference pixels are partially available.

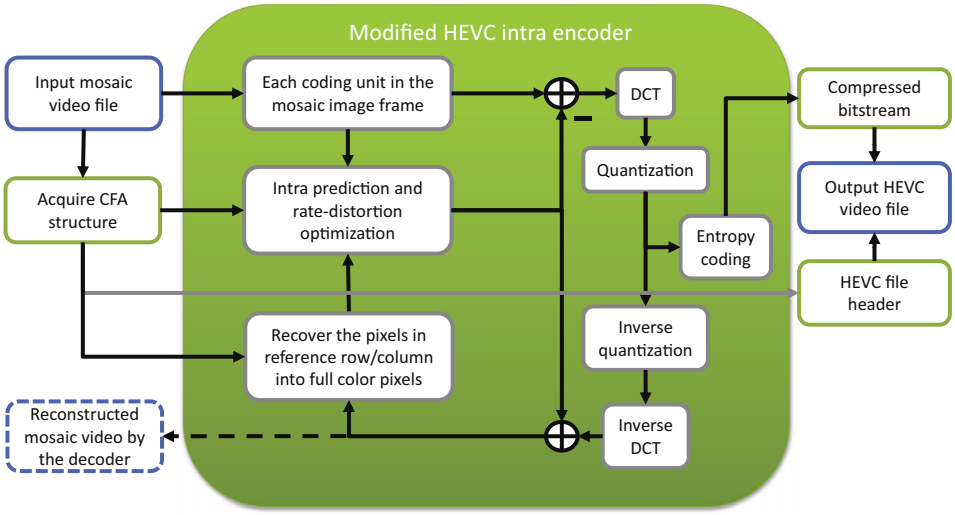

Fig. 6. Flowchart of the proposed universal intra coding scheme for arbitrary RGB-CFAs in HEVC.

For predicting the luma values in a prediction unit, the HEVC standard develops 35 intra prediction modes, whereas only 9 of those are available in H.264/AVC, and hence HEVC can predict complex structures more accurately. The 35 intra prediction modes in HEVC are labeled as modes $0, 1, \ldots$, and 34 in Fig. 3 and are available for five different-sized prediction units.

Given an $N \times N$ prediction unit $P^{i,j}_{N\times N}$ with $j = 0$ for $N = 64, 32, 16, 8$ and $j = 0, 1, 2, 3$ for $N = 4$, to predict the luma value for each pixel in $P^{i,j}_{N\times N}$, HEVC first forms a set S of reference pixels which are collected from the neighboring encoded pixels, including the left, upper left, upper, upper right, and lower left regions of $P^{i,j}_{N\times N}$. As shown in Fig. 4(a), S is the set $\{s_{0,0}, s_{0,1}, \ldots, s_{0,2N}, s_{1,0}, s_{2,0}, \ldots, s_{2N,0}\}$ where $s_{0,k}$ is the kth reference pixel in the reference row above the current prediction unit and $s_{k,0}$ is the kth reference pixel in the reference column to the left of the current prediction unit. Note that in Fig. 4(b), the neighboring pixels $s_{N+1,0}, s_{N+2,0}, \ldots, s_{2N,0}$ from the lower left region can not be included in S since they are not yet encoded by HEVC. Once the set S of reference pixels corresponding to the current prediction unit $P^{i,j}_{N\times N}$ is obtained, each intra prediction mode shown in Fig. 3 is adopted to predict the luma value for each pixel in the current prediction unit (Fig. 5).

The 35 intra prediction modes in HEVC can be divided into three categories: DC mode, planar mode, and the prediction modes with direction. The DC mode is often selected when there exists little variation on the luma values in the prediction unit. The DC mode (i.e., mode 2 in Fig. 3) uses an average luma value of reference pixels to predict the luma value for pixel $x_{m,n}$ in the current prediction unit where the predicted luma value can be expressed as

$$\hat{L}(x_{m,n}) = \frac{\sum_{k=1}^{N}(L(s_{0,k}) + L(s_{k,0}))}{2N}, \quad m, n \in \{1, 2 \ldots, N\}, \tag{1}$$

with $L(s_{k,0})$ and $L(s_{0,k})$ denoting, respectively, the luma values of the left and upper reference pixels. When there exists gradual changes of the luma values in the prediction unit, the planar mode is appropriate for prediction. The planar mode (i.e., mode 34 in Fig. 3) predicts the luma value by the average of the horizontal and vertical linear interpolations where the interpolation weights are inversely proportional to the distances between the target pixel and the horizontal and vertical reference pixels. The predicted luma value of $x_{m,n}$ by planar mode can be expressed by

$$\begin{aligned}\hat{L}(x_{m,n}) = {} & \frac{1}{2}\left\{\frac{N-n}{N} \times L(s_{m,0}) + \frac{n}{N} \times L(s_{0,N+1})\right\} \\ & + \frac{1}{2}\left\{\frac{N-m}{N} \times L(s_{0,n}) + \frac{m}{N} \times L(s_{N+1,0})\right\}.\end{aligned} \tag{2}$$

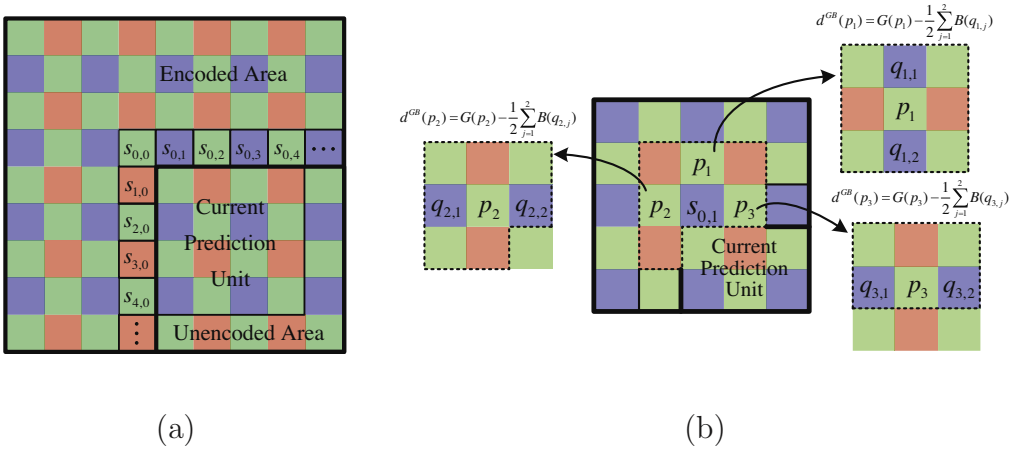

Fig. 7. An example of recovering the missing green color value for a reference pixel using the proposed modified universal demosaicing method. (For interpretation of the references to color in this figure legend, the reader is referred to the web version of this article.)

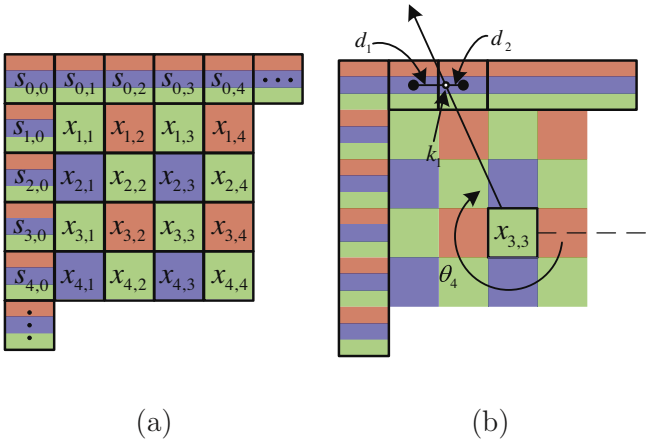

Fig. 8. An example of obtaining the predicted green color value for a pixel with green color value given the demosaiced reference pixels. (For interpretation of the references to color in this figure legend, the reader is referred to the web version of this article.)

In addition to DC and planar modes, the rest of prediction modes consider 33 different directions to predict the luma value for the target pixel in the current prediction unit. The prediction mode with some specific direction is often used to capture the characteristics of edges in the prediction unit. When applying the prediction mode with direction θ_d which is the rotation angle clockwise from the horizontal axis to the ray labeled with number d in Fig. 3, the ray emitted from the target pixel intersects (may intersect) the reference row above or the reference column left to the prediction unit. Then the weighted average of the luma values corresponding to two reference pixels next to the intersection can be used to predict the luma value of the target pixel. Denoting, respectively, by $\lfloor\cdot\rfloor$ and $\lceil\cdot\rceil$ the floor and ceiling functions, the predicted luma value of the target pixel by the prediction mode with direction θ_d can be expressed as

$$\hat{L}(x_{m,n}) = \begin{cases} w_1 \times L(s_{0,\lfloor k_1 \rfloor}) + (1-w_1) \times L(s_{0,\lceil k_1 \rceil}), \\ \text{if } \theta_d \geqslant 3\pi/2 \text{ or } \tan\theta_d \geqslant m/n \text{ for } \pi \leqslant \theta_d < 3\pi/2, \\ w_2 \times L(s_{\lfloor k_2 \rfloor,0}) + (1-w_2) \times L(s_{\lceil k_2 \rceil,0}), \text{ otherwise}, \end{cases} \tag{3}$$

where $k_1 = n - m/\tan\theta_d$, $k_2 = m - n\tan\theta_d$, $w_1 = 1 - (k_1 - \lfloor k_1 \rfloor)$, and $w_2 = 1 - (k_2 - \lfloor k_2 \rfloor)$.

Since the intra prediction for chroma values of pixels in each prediction unit is similar to the intra prediction for luma values, the detailed prediction procedure for chroma values is omitted. Furthermore, since this research is focused on the intra prediction, the inter prediction scheme is not discussed in this paper.

To determine the optimal luma intra prediction mode for each prediction unit, the RD cost corresponding to each luma intra prediction mode is calculated and the one with the minimum RD cost is selected as the optimal luma intra prediction mode. Similarly, the optimal chroma intra prediction mode is determined for each prediction unit. Once the optimal luma and chroma intra prediction modes for each prediction unit are determined, the RD cost associated with the prediction unit is calculated as the sum of the RD costs corresponding to the optimal luma and chroma modes.

Given the RD cost for each prediction unit, we can obtain the RD cost associated with each coding unit in Fig. 2. The hierarchical structure corresponding to the coding unit $C^0_{64\times64}$ in Fig. 2 will be pruned and merged according to the RD optimization procedure and hence the optimal intra coding partition corresponding to $C^0_{64\times64}$ can be determined.

3. The proposed universal intra coding scheme for arbitrary RGB-CFAs in HEVC

In this section, we propose a two-stage universal intra coding scheme for compressing mosaic video sequences with arbitrary RGB-CFAs in HEVC. The proposed universal intra coding scheme can be divided into two stages: the modified universal demosaicing stage for reference pixels and the color selection-based intra prediction stage for mosaic pixels. The complete flowchart of the proposed scheme is shown in Fig. 6.

To compress one mosaic video sequence using the proposed universal intra coding scheme, we need to acquire the mosaic structure used in the video sequence in advance. In general, the mosaic structure used can be obtained from either the camera manufacturers if the compression is implemented in the camera, or the raw CFA video sequence stored in TIFF-EP format if the compression is implemented in a companion PC [15,16]. However, in practice, the mosaic structure used may not be available. To tackle this problem, we develop an algorithm to identify the mosaic structure used. Considering pixel p with color component $C \in \{R, G, B\}$, denote by $C(p)$ the color value of pixel p. Under the assumption that the video has CFA structure j, let $\mathbb{S}^C_j(p)$ represent the set of pixels which fall in the window centered at p and have the identical color component C. When the CFA structure used is not available, choose the CFA structure j^* such that the total average square difference, over all concerned windows and three identical color components, is minimized; that is,

$$j^* = \arg\min_{j\in J} \sum_{p\in V} \sum_{q\in\mathbb{S}^C_j(p)} \frac{(C(p)-C(q))^2}{|\mathbb{S}^C_j(p)|}, \tag{4}$$

where V represents the set of pixels in the images of the video and J is the set of 10 commonly used CFA structures as shown in Fig. 1. The performance of the algorithm for identifying the CFA structure is given in Section 4.3.

Once the mosaic structure is known or identified, the proposed two-stage universal intra coding scheme is used to compress the input mosaic video sequence. The proposed intra coding scheme first demosaics the reference pixels and then performs the intra prediction using the demosaiced reference pixels. We first describe

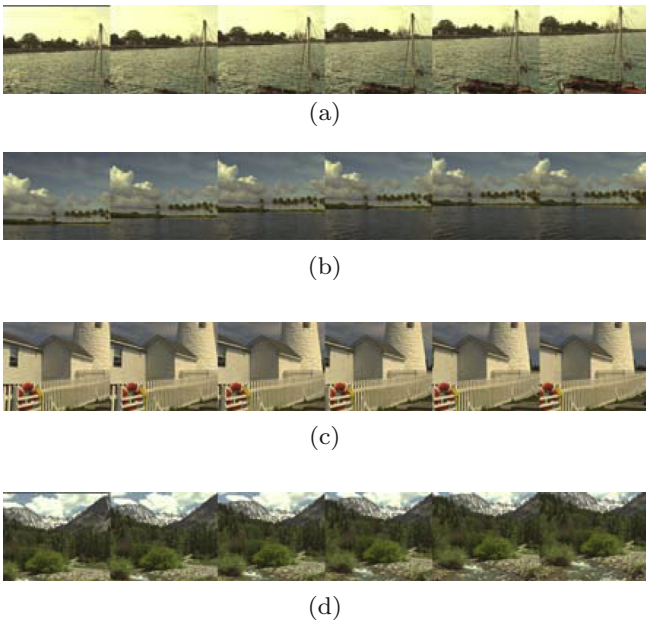

Fig. 9. Four test video sequences: (a) Boat, (b) Island, (c) Lighthouse and (d) Nature.

the universal demosaicing scheme for reference pixels, which is a modification of Yang et al.'s universal demosaicing method. The universal demosaicing method by Yang et al.'s recovers the missing color values for each pixel by referring to all the neighboring mosaic pixels. For demosaicing reference pixels in the first stage of the proposed scheme, directly applying Yang et al.'s demosaicing method may result in fatal errors since the unencoded pixels are referenced. Thus, when demosaicing reference pixels in the first stage of the proposed scheme, we modified Yang et al.'s universal demosaicing method such that only encoded pixels are referenced when recovering the missing color values for reference pixels.

When demosaicing reference pixel t with color component $C \in \{R, G, B\}$, let $\mathbb{W}^C(t)$ denote the set of encoded pixels with color component C which fall in the window centered at t. Increase the window size from 3×3 until there exist at least two pixels in $\mathbb{W}^C(t)$. Since most pixels in the mosaic images with commonly used CFA structures have G color component, we first recover the reference pixels with missing G color component. If the reference pixel has blue color value, its green color value is recovered by considering the difference between the green and blue color values of the neighboring encoded pixels; that is,

$$G(t) = B(t) + \sum_{p \in \mathbb{W}^G(t)} w^{GB}(p) d^{GB}(p), \tag{5}$$

where

$$d^{GB}(p) = G(p) - \frac{1}{|\mathbb{W}^B(p)|} \sum_{q \in \mathbb{W}^B(p)} B(q)$$

represents the difference between the green color value of the neighboring encoded pixel p and the average blue color value of its neighboring encoded pixels and the weight

$$w^{GB}(p) = \frac{1 \Big/ \left(1 + \sum_{q \in \mathbb{W}^G(t)} \left| d^{GB}(p) - d^{GB}(q) \right| \right)}{\sum_{s \in \mathbb{W}^G(t)} \left[1 \Big/ \left(1 + \sum_{q \in \mathbb{W}^G(t)} \left| d^{GB}(s) - d^{GB}(q) \right| \right) \right]} \tag{6}$$

is vaguely proportional to the similarity of $d^{GB}(p)$.

Similarly, if the reference pixel has red color value, its green color value is recovered by considering the difference between the green and red color values of the neighboring encoded pixels; that is,

$$G(t) = R(t) + \sum_{p \in \mathbb{W}^G(t)} w^{GR}(p) d^{GR}(p), \tag{7}$$

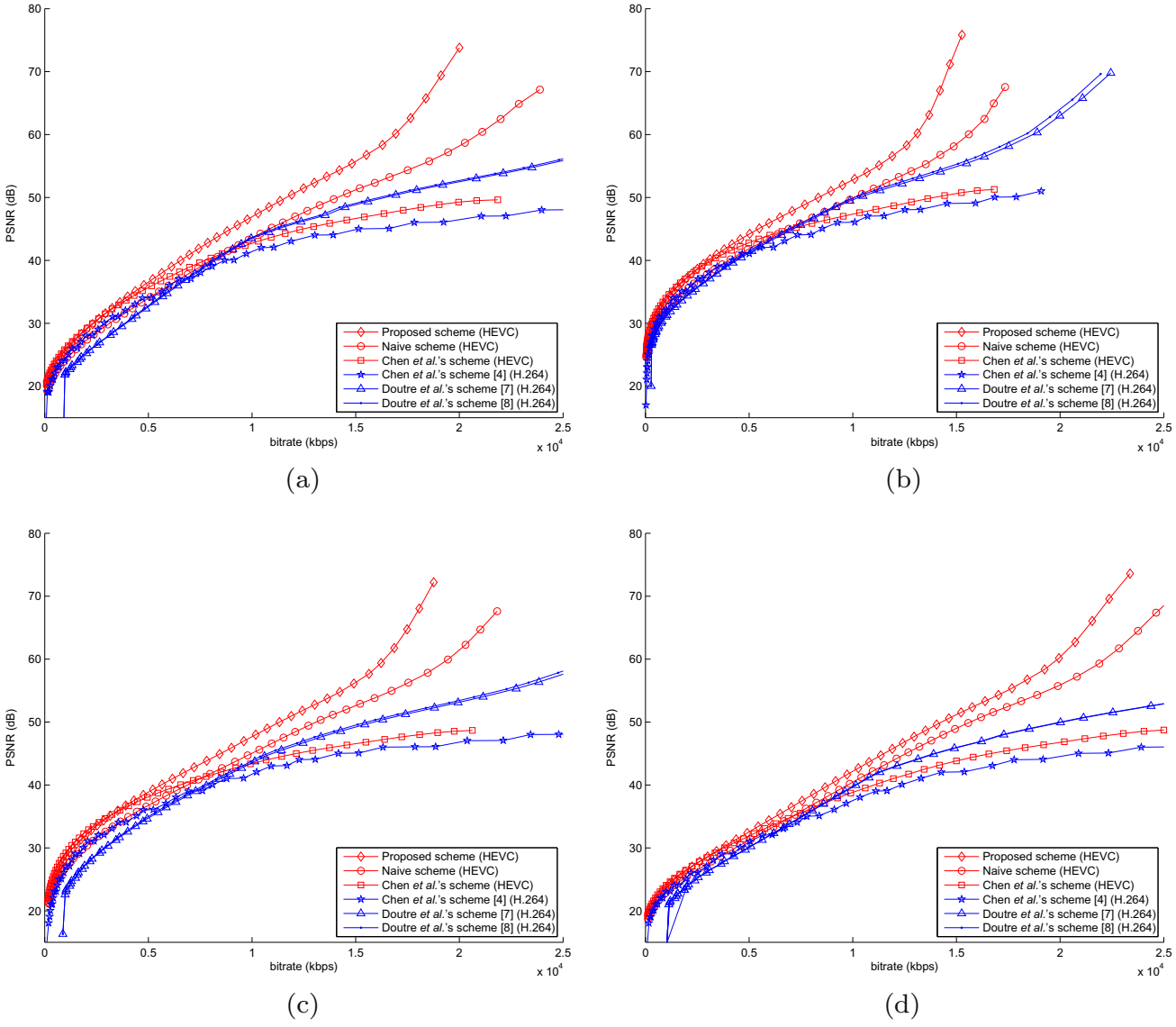

Fig. 10. Under the Bayer CFA, RD curves corresponding to different intra coding schemes for video sequences (a) Boat, (b) Island, (c) Lighthouse and (d) Nature.

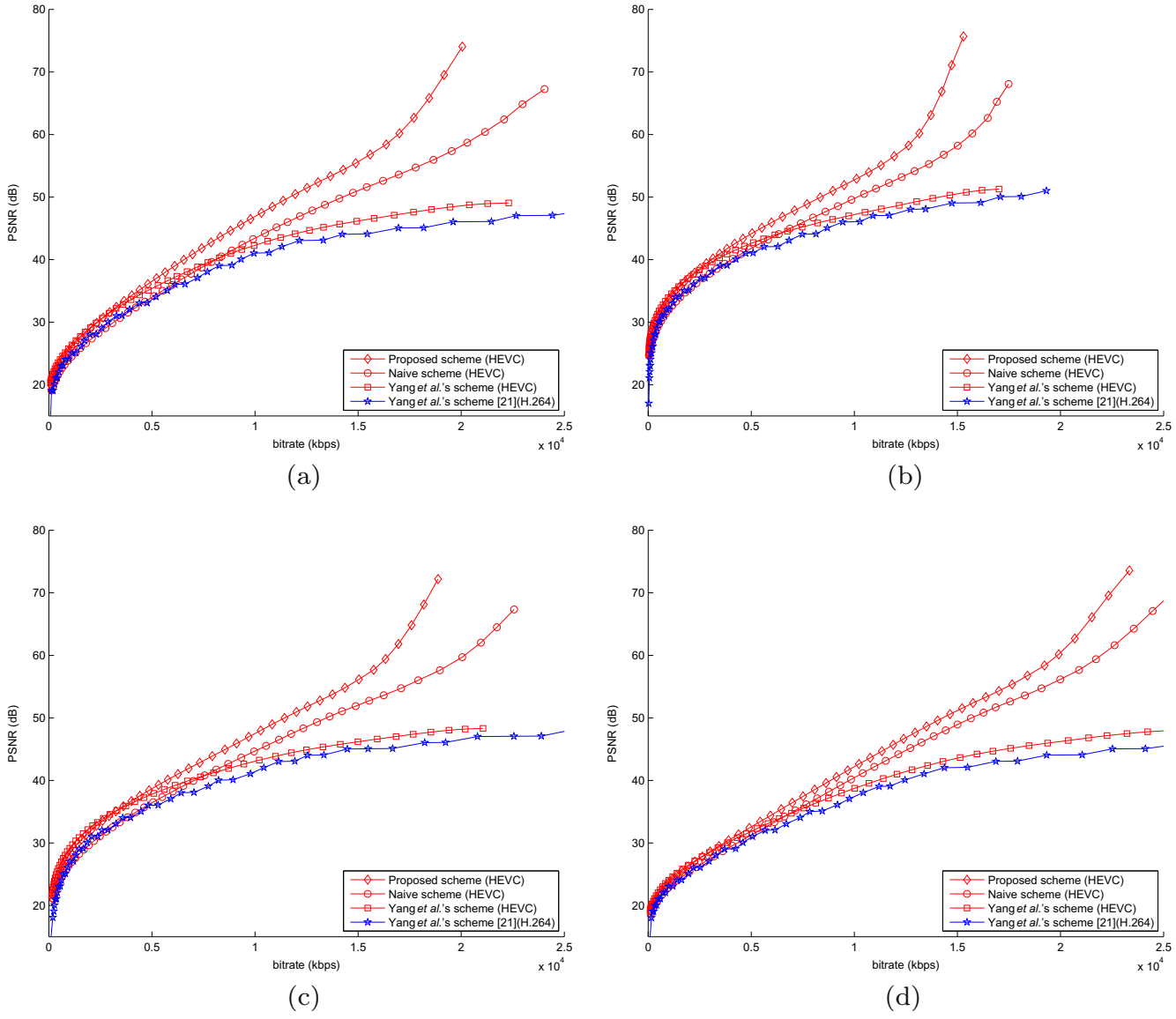

Fig. 11. Under the Lukac and Plataniotis CFA, RD curves corresponding to different intra coding schemes for video sequences (a) Boat, (b) Island, (c) Lighthouse and (d) Nature.

where

$$d^{GR}(p) = G(p) - \frac{1}{|\mathbb{W}^R(p)|}\sum_{q\in\mathbb{W}^R(p)} R(q)$$

and

$$w^{GR}(p) = \frac{1\Big/\left(1+\sum_{q\in\mathbb{W}^G(t)}\left|d^{GR}(p)-d^{GR}(q)\right|\right)}{\sum_{s\in\mathbb{W}^G(t)}\left[1\Big/\left(1+\sum_{q\in\mathbb{W}^G(t)}\left|d^{GR}(s)-d^{GR}(q)\right|\right)\right]}. \quad (8)$$

To better understand the above algorithm, we present an example of recovering the missing green color value for a reference pixel using the proposed modified universal demosaicing method. Fig. 7(a) shows a prediction unit of size 4×4 and the neighboring reference pixels in a mosaic image frame with the Bayer CFA structure. Consider recovering the missing green color value for the reference pixel $s_{0,1}$ which has the blue component. First identify, within the window of size 3×3 centered at pixel $s_{0,1}$, the encoded pixels p_1, p_2, and p_3 with the green component, as shown in Fig. 7(b). For each p_i, find, within the 3×3 window centered at p_i, the encoded pixels with blue component and then compute the average of these blue color values and obtain the difference $d^{GB}(p_i)$ between the green color value of p_i and this average blue color value. Thus the recovered green color value for reference pixel $s_{0,1}$ is obtained by

$$G(s_{0,1}) = B(s_{0,1}) + \sum_{i=1}^{3} w^{GB}(p_i)d^{GB}(p_i),$$

where weight $w^{GB}(p_i)$ is vaguely proportional to the similarity of $d^{GB}(p_i)$, as shown in Eq. (6).

Once the missing green color values of the reference pixels in the reference row and column are recovered, the missing red or blue color values of reference pixels can be recovered. Based on the encoded or recovered green color value of the reference pixel t, the missing red color value of the reference pixel t can be recovered by

$$R(t) = G(t) + \sum_{p\in\mathbb{W}^R(t)} w^{RG}(p)d^{RG}(p), \quad (9)$$

where $d^{RG}(p) = R(p) - G(p)$ and $w^{RG}(p)$ is defined like Eq. (6). Similarly, the missing blue color value of the reference pixel t can be recovered by

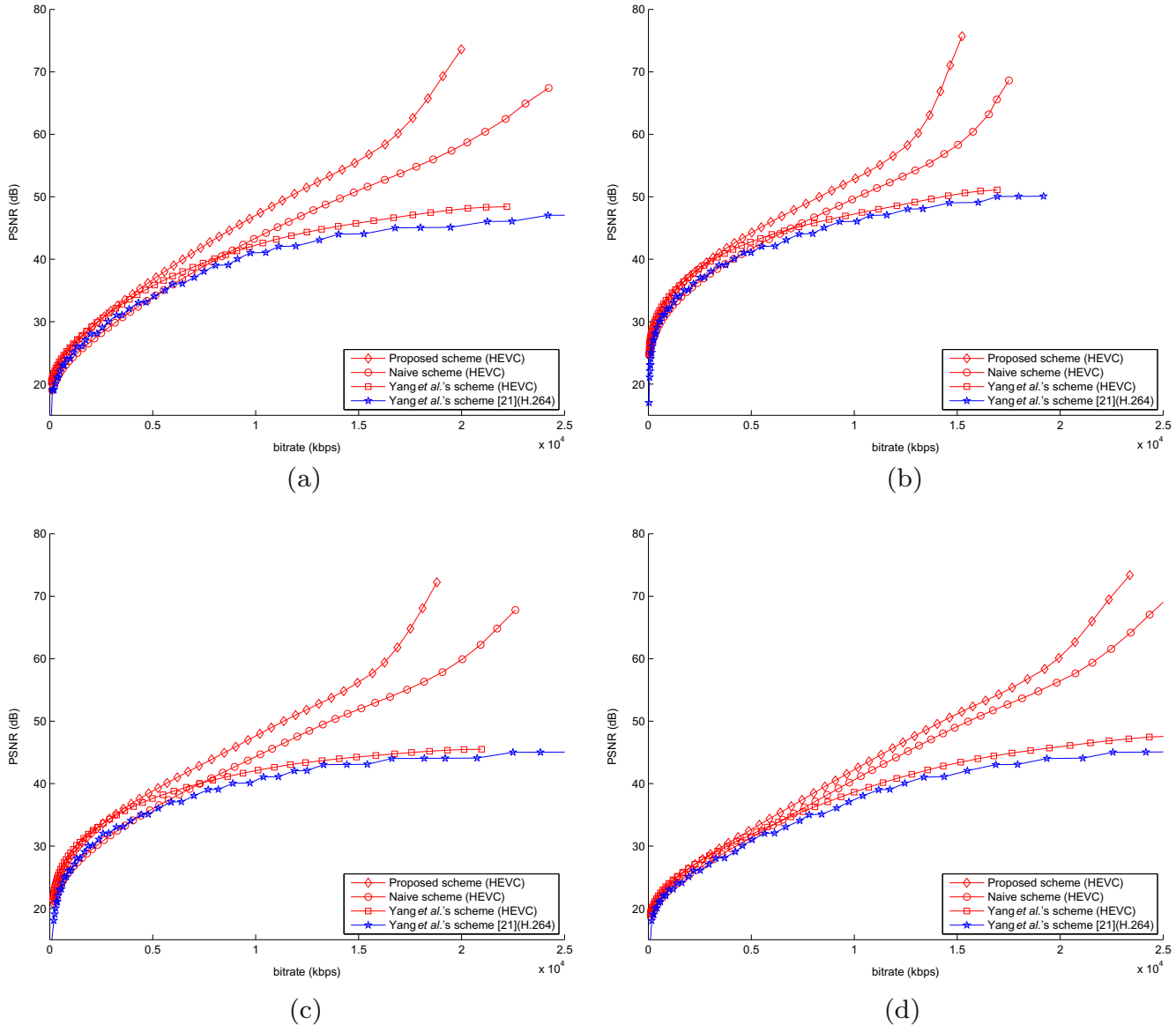

Fig. 12. Under the Yamanaka CFA, RD curves corresponding to different intra coding schemes for video sequences (a) Boat, (b) Island, (c) Lighthouse and (d) Nature.

$$B(t) = G(t) + \sum_{p \in \mathbb{W}^B(t)} w^{BG}(p) d^{BG}(p), \tag{10}$$

where $d^{BG}(p) = B(p) - G(p)$ and $w^{BG}(p)$ is defined like Eq. (6).

Once the color values of the missing color components in reference pixels are recovered through the above modified demosaicing process, the proposed color selection-based intra prediction stage can be initiated to predict the color value of the corresponding color component for each mosaic pixel in the current prediction unit.

Consider intra prediction for prediction unit $P^{i,j}_{N\times N}$ with $i = 0, 1, \ldots, (64/N)^2 - 1$; $j = 0$ for $N = 64, 32, 16, 8$; $j = 0, 1, 2, 3$ for $N = 4$. When there exists little variation of the color values in the prediction unit, the intra mode selection scheme prefers the DC prediction mode to the other modes. For pixel $x_{m,n}$ with color component C, $C \in \{R, G, B\}$, the predicted color value using DC mode is expressed as

$$\hat{C}(x_{m,n}) = \frac{\sum_{k=1}^{N} (C(s_{0,k}) + C(s_{k,0}))}{2N}, \tag{11}$$

where $C(s_{k,0})$ and $C(s_{0,k})$ represent, respectively, the C color values of the pixels $s_{k,0}$ and $s_{0,k}$ in the left reference column and upper reference row, respectively.

When there exists gradual changes of the color values in the prediction unit, the planar prediction mode is preferred. Planar intra prediction mode exploits the color values of the reference pixels closest to the pixel to be predicted and the predicted color value can be expressed as

$$\begin{aligned}\hat{C}(x_{m,n}) = {} & \frac{1}{2}\left\{\frac{N-n}{N} \times C(s_{m,0}) + \frac{n}{N} \times C(s_{0,N+1})\right\} \\ & + \frac{1}{2}\left\{\frac{N-m}{N} \times C(s_{0,n}) + \frac{m}{N} \times C(s_{N+1,0})\right\}.\end{aligned} \tag{12}$$

When there exists edges in the prediction unit, the prediction mode with some direction is appropriate for capturing the characteristics of edges. When using the prediction mode with direction θ_d, the predicted C color value of $x_{m,n}$ can be expressed as

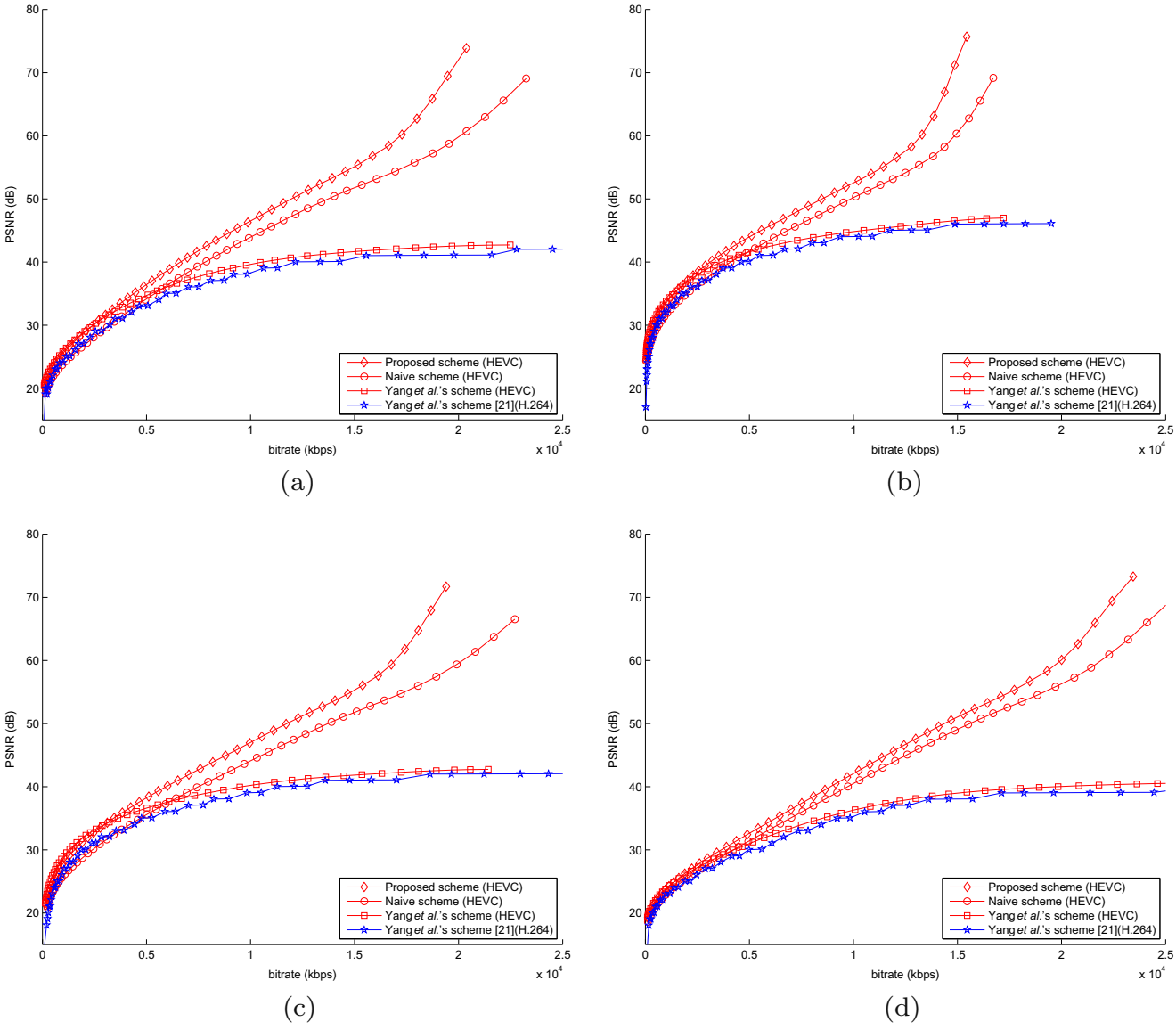

Fig. 13. Under the diagonal stripe CFA, RD curves corresponding to different intra coding schemes for video sequences (a) Boat, (b) Island, (c) Lighthouse and (d) Nature.

$$\hat{C}(x_{m,n}) = \begin{cases} w_1 \times C(s_{0,\lfloor k_1 \rfloor}) + (1-w_1) \times C(s_{0,\lceil k_1 \rceil}), \\ \text{if } \theta_d \geqslant 3\pi/2 \text{ or } \tan\theta_d \geqslant m/n \text{ for } \pi \leqslant \theta_d < 3\pi/2, \\ w_2 \times C(s_{\lfloor k_2 \rfloor,0}) + (1-w_2) \times C(s_{\lceil k_2 \rceil,0}), \text{ otherwise}, \end{cases} \tag{13}$$

where k_1, k_2, w_1, and w_2 have the same definitions as mentioned in Eq. (3).

To better understand the proposed color selection-based intra prediction method, we present an example to illustrate how to obtain the predicted green color value for a pixel with green color value given the demosaiced reference pixels. Fig. 8(a) shows a prediction unit of size 4×4 and the neighboring demosaiced reference pixels in a mosaic image frame with the Bayer CFA structure. Suppose the intra prediction mode with direction θ_4 as shown in Fig. 3 is selected to predict the green color value for pixel $x_{3,3}$ which has green color value. Determine the reference pixels $s_{0,1}$ and $s_{0,2}$ which are next to the intersection $k_1 = 1.78125$ of the ray emitted from pixel $x_{3,3}$ with direction θ_4 and the reference row, as shown in Fig. 8(b). The predicted green color value $\hat{G}(x_{3,3})$ for $x_{3,3}$ is the weighted average of the green color values of $s_{0,1}$ and $s_{0,2}$; that is,

$$\hat{G}(x_{3,3}) = \frac{d_2}{d_1+d_2} \times G(s_{0,1}) + \frac{d_1}{d_1+d_2} \times G(s_{0,2}),$$

where $d_1 = k_1 - \lfloor k_1 \rfloor = 0.78125$ and $d_2 = \lceil k_1 \rceil - k_1 = 0.21875$ are the distances between the intersection and the reference pixels $s_{0,1}$ and $s_{0,2}$, respectively.

In the proposed second stage, instead of determining to which case the prediction unit belongs according to its content, the RD costs associated with 35 intra prediction modes will be calculated and the prediction mode with the minimum RD cost is regarded as the best and is selected for intra prediction. After intra prediction for the prediction unit, the prediction residuals are encoded by the discrete cosine transform-based coding technique and the encoded residuals are transferred to the decoder side for reconstructing the mosaic video sequence.

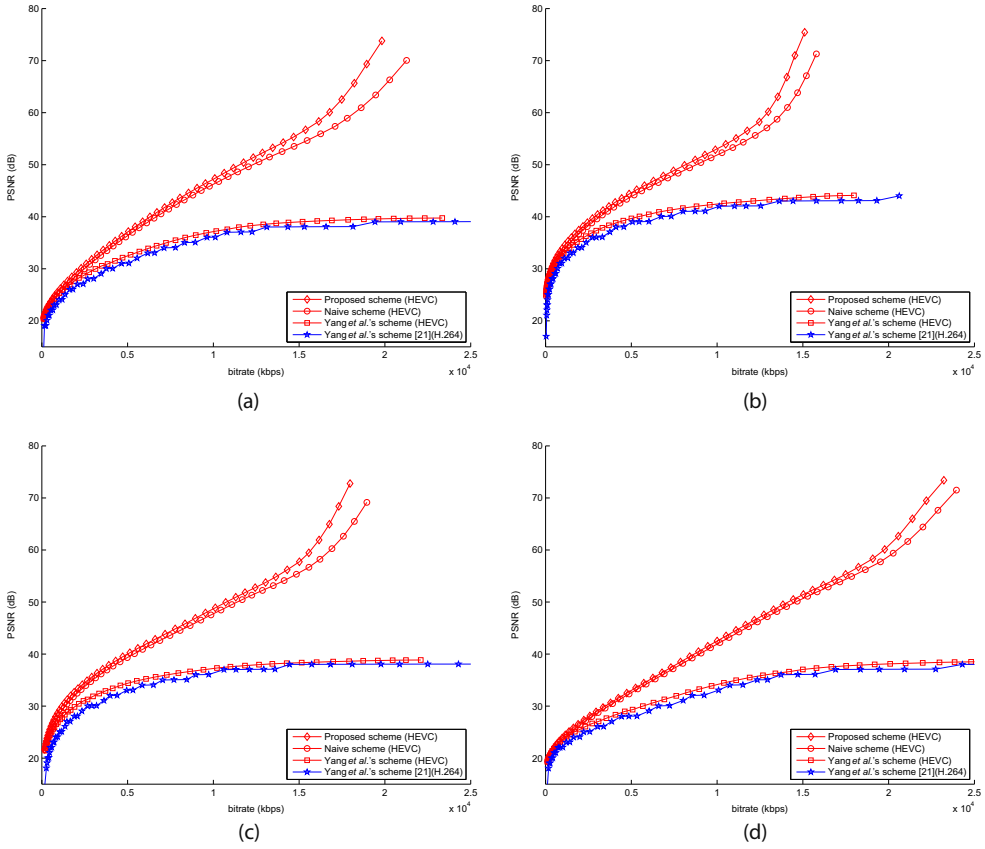

Fig. 14. Under the vertical stripe CFA, RD curves corresponding to different intra coding schemes for video sequences (a) Boat, (b) Island, (c) Lighthouse and (d) Nature.

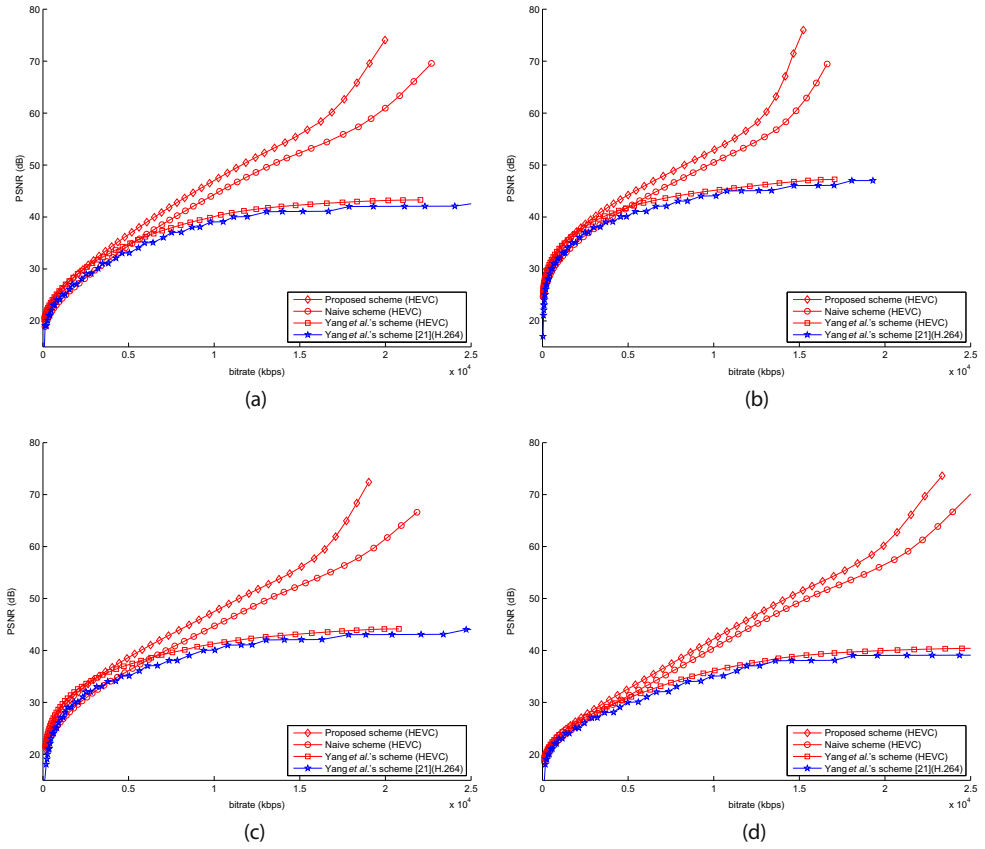

Fig. 15. Under the modified Bayer CFA, RD curves corresponding to different intra coding schemes for video sequences (a) Boat, (b) Island, (c) Lighthouse and (d) Nature.

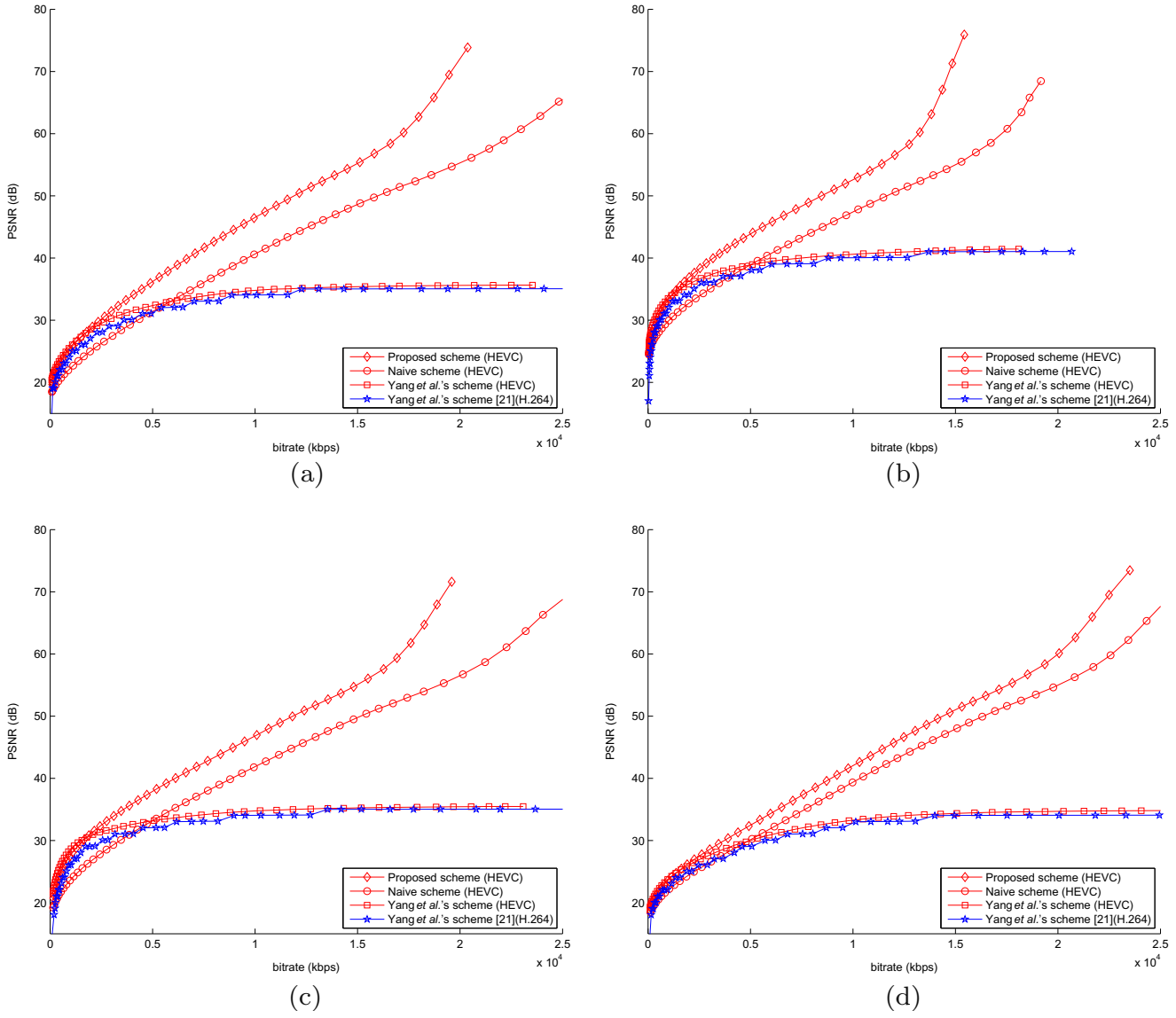

Fig. 16. Under the HVS-based CFA, RD curves corresponding to different intra coding schemes for video sequences (a) Boat, (b) Island, (c) Lighthouse and (d) Nature.

4. Experimental results

This paper presents a two-stage universal intra coding scheme for compressing mosaic video sequences with arbitrary RGB-CFAs in HEVC. Since the proposed intra coding scheme is the first intra coding scheme for compressing mosaic video sequences in HEVC, the conventional intra coding schemes for compressing mosaic video sequences are adapted, if possible, to the HEVC standard. Furthermore, the experiments of applying the conventional intra coding schemes for compressing mosaic video sequences in H.264/AVC are performed for comparison.

Since most conventional intra coding schemes are designed for compressing mosaic video sequences with the Bayer CFA structure, both the mosaic video sequences with the Bayer CFA structure and the other nine non-Bayer CFA structures are considered for comparison. For compressing mosaic video sequences with the Bayer CFA structure, the intra coding schemes by Doutre et al. [7,8] and Chen et al. [4] in H.264/AVC are considered for comparison where the intra coding scheme by Chen et al. [4] is further adapted to the HEVC standard. As for mosaic video sequences with non-Bayer CFA structures, the intra coding scheme by Yang et al. [21], which is universal in H.264/AVC, is adapted to the HEVC standard for comparison.

In addition, for mosaic video sequences with the Bayer and non-Bayer CFA structures, the second stage of the proposed intra coding scheme predicts the color value for each mosaic pixel based on the color values of the identical color component associated with the reference pixels which are demosaiced in the first stage. If the reference pixels are not demosaiced, a naive approach as an alternative for the second-stage prediction of the proposed scheme is to predict the color value for each mosaic pixel based on the color values of any color component associated with the non-demosaiced reference pixels. Contrasted to the proposed scheme, this naive approach ignores the correlation among pixels with identical color components for intra coding by treating the mosaic video sequences as gray-level video sequences. Comparing the proposed scheme with the naive approach reveals the gains from demosaicing the reference pixels in the first stage.

Four test video sequences with full RGB colors, adopted from the website [28], are shown in Fig. 9. Each test video sequence has 50 frames and each frame has spatial resolution of 352×288. For each test video sequence, subsample, according to

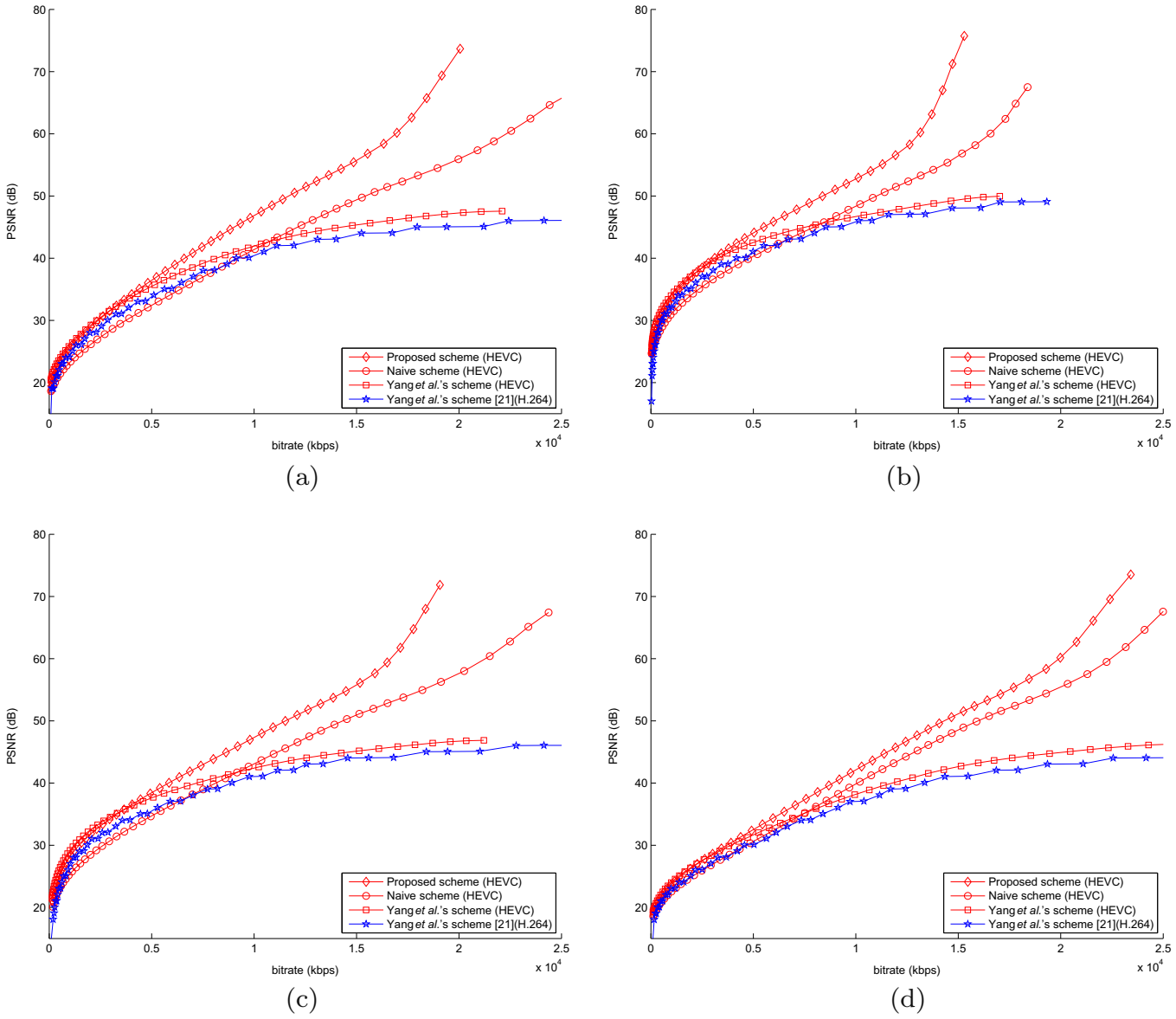

Fig. 17. Under the type I pseudo-random CFA, RD curves corresponding to different intra coding schemes for video sequences (a) Boat, (b) Island, (c) Lighthouse and (d) Nature.

the specific RGB-CFA structure, appropriate color for each pixel to generate the input mosaic video sequences with the Bayer CFA and nine non-Bayer CFA structures, as shown in Fig. 1. The compression platforms used are JM 18.4 and HM 4.0 for H.264/AVC-based and HEVC-based intra coding schemes, respectively. The intra coding schemes and both compression platforms were realized in Visual C++ 2008 and implemented on the IBM compatible computer with Intel i7-3770 CPU 3.4 GHz, 16 GB RAM, and Microsoft Windows 7 64-bit operating system.

4.1. Performance evaluation metrics

The quality of the reconstructed video sequence and the storage requirement are the main performance measures for comparison. High quality of the reconstructed video sequence is often associated with large storage requirement. The rate-distortion (RD) curve which measures the tradeoff between the quality and the storage for each intra coding scheme is constructed for comparison. Furthermore, the relative gain, measured by Bjøntegaard delta peak signal-to-noise ratio (BD-PSNR) and Bjøntegaard delta bitrate (BD-BR) [2], of the proposed universal intra coding scheme over each of the existing intra coding schemes is calculated.

For the quality of the reconstructed video sequence, we compute the PSNR of the reconstructed mosaic video sequence, which is the average of 50 PSNR values corresponding to 50 mosaic image frames in the reconstructed video sequence. Denote by $\mathbb{P} = \{(m,n)|0 \leqslant m \leqslant H-1,\ 0 \leqslant n \leqslant W-1\}$ the set of pixel coordinates in one test mosaic image frame of size $W \times H$. The PSNR of the reconstructed video sequence with N mosaic image frames is expressed as

$$\mathrm{PSNR} = \frac{1}{N}\sum_{i=1}^{N} 10\log_{10}\frac{255^2}{\mathrm{MSE}_i}, \tag{14}$$

with

$$\mathrm{MSE}_i = \frac{1}{WH}\sum_{p\in\mathbb{P}}\left[C_i(p) - \tilde{C}_i(p)\right]^2, \tag{15}$$

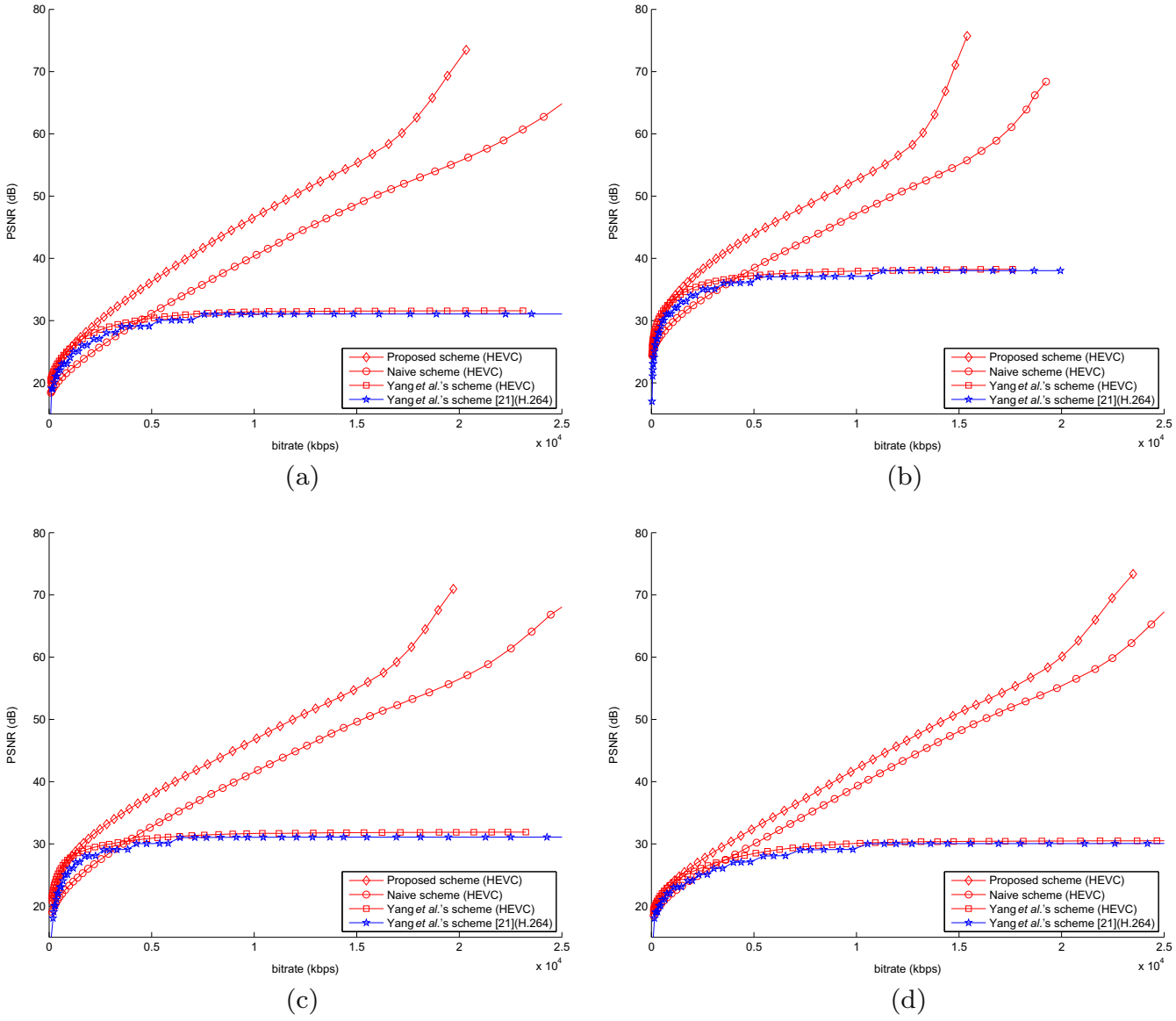

Fig. 18. Under the type II pseudo-random CFA, RD curves corresponding to different intra coding schemes for video sequences (a) Boat, (b) Island, (c) Lighthouse and (d) Nature.

where $C_i(p)$ denotes the color value of the pixel at position p in mosaic image frame i and $\tilde{C}_i(p)$ represents the reconstructed analogue. Higher values of PSNR indicate better quality of the reconstructed video sequence. With the frame rate of F frames per second, the bitrate of the compressed mosaic video sequence is defined as

$$\text{bitrate} = \frac{T}{N} \times F, \tag{16}$$

where T represents the total number of bits used for compressing the mosaic video sequence with N frames. Low bitrate implies less requirement for storage and network bandwidth and is preferred.

Since higher values of PSNR are often associated with higher values of bitrate, the RD curve which plots PSNR against bitrate measures the tradeoff and is used to illustrate the overall performance of an intra coding scheme. For plotting the RD curves, all the quantization parameters (QPs) from 1 to 51 are used in the experiment to obtain the corresponding values of PSNR and bitrate. Detailed experimental results are available in [28].

Furthermore, indices BD-PSNR and BD-BR which measure, respectively, the relative gains on PSNR and bitrate of one intra coding scheme over another intra coding scheme are calculated to provide quantitative comparison results. We calculate the BD-PSNR and BD-BR for the proposed intra coding scheme over each compared intra coding scheme. Indices BD-PSNR and BD-BR essentially measure, respectively, the average differences in PSNR and bitrate of two RD curves. Positive values in BD-PSNR and negative values in BD-BR indicate that the proposed intra coding scheme performs better. Since RD curves may not have identical starting and ending points, the range over which the BD-PSNR is calculated is the intersection of the supports of all the RD curves. The range for calculating BD-BR is determined similarly.

4.2. Performance comparison of intra coding schemes

The RD curves of the intra coding schemes for the Bayer CFA and non-Bayer CFA structures are given in Fig. 10 and Figs. 11–19,

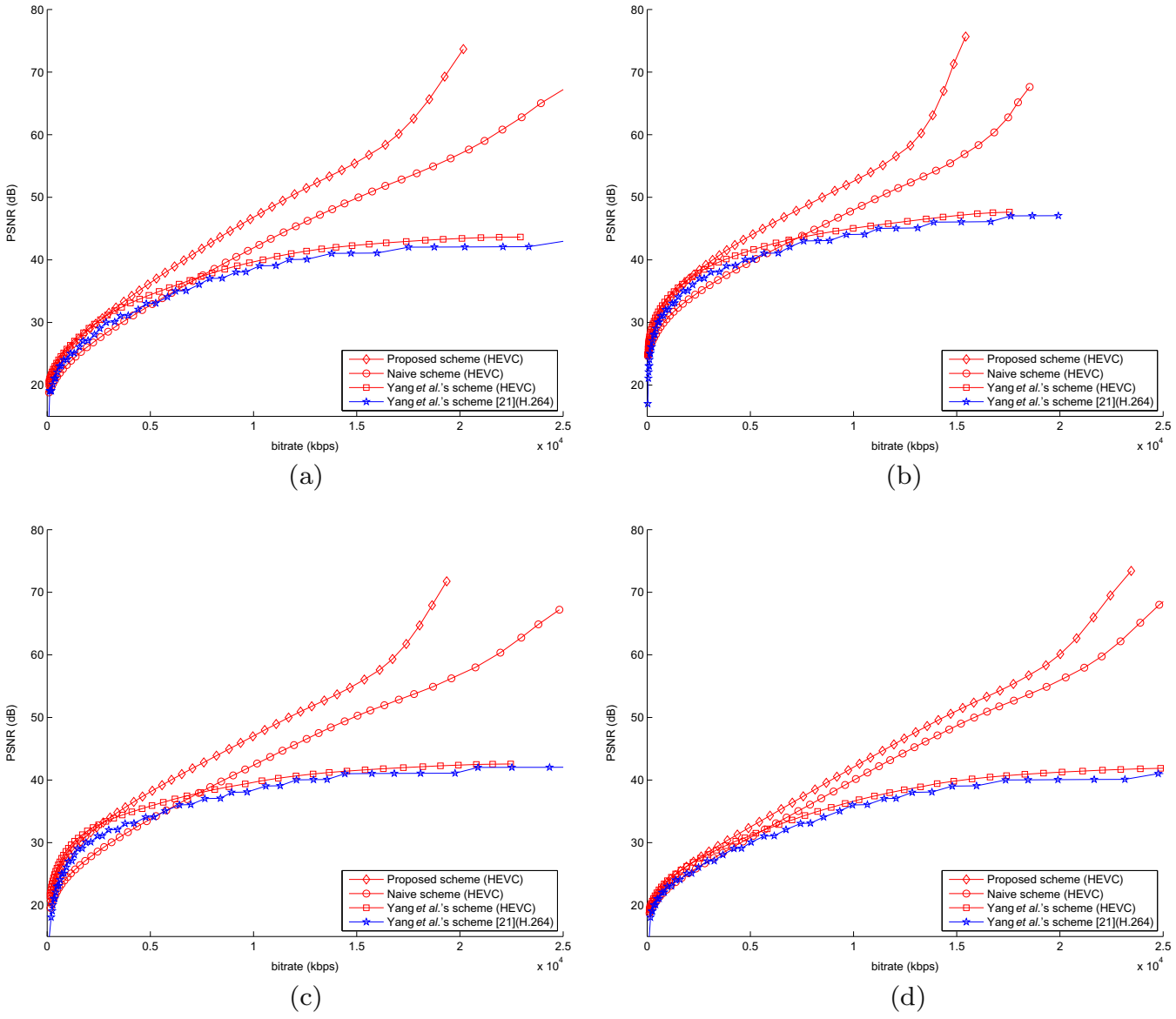

Fig. 19. Under the type III pseudo-random CFA, RD curves corresponding to different intra coding schemes for video sequences (a) Boat, (b) Island, (c) Lighthouse and (d) Nature.

respectively. The RD curves in Fig. 10 show that, when compressing mosaic video sequences with the Bayer CFA structure, the proposed intra coding scheme achieves the best compression performance and the naive approach which treats the input mosaic video sequence as a grey-level video sequence dominates other intra coding schemes. For test video sequences "Boat," "Island," and "Lighthouse," the bitrates for intra coding schemes by Doutre et al. [7,8], which converts CFA structure into three distinct color planes, increase significantly for high values of PSNR. The reason for significant increase in bitrate is because the intra prediction in the schemes by Doutre et al. [7,8] results in large prediction residuals due to the distortion of relative arrangement of green color components; as for sequence "Nature", no similar result is observed since their intra coding schemes cannot deliver the compression results

Table 1
BD-PSNR (in dB) of the proposed scheme over each compared scheme under the Bayer CFA.

Video sequence	Bitrate range	Doutre et al.'s intra coding scheme [7] (H.264) BD-PSNR	Doutre et al.'s intra coding scheme [8] (H.264) BD-PSNR	Chen et al.'s intra coding scheme [4] (H.264) BD-PSNR	Chen et al.'s intra coding scheme (HEVC) BD-PSNR	Naive intra coding scheme (HEVC) BD-PSNR
Boat	911.8–20001.2	8.59	8.47	7.05	5.40	5.38
Island	271.2–15265.6	6.86	6.68	6.43	4.45	4.32
Lighthouse	876.1–18763.2	7.95	7.74	6.38	4.17	3.87
Nature	1039.3–23372.1	7.55	7.49	7.26	6.07	3.82
Average	BD-PSNR	7.74	7.59	6.78	5.02	4.34

Table 2
BD-BR (in %) of the proposed scheme over each compared scheme under the Bayer CFA.

Video sequence	PSNR range	Doutre et al.'s intra coding scheme [7] (H.264) BD-BR	Doutre et al.'s intra coding scheme [8] (H.264) BD-BR	Chen et al.'s intra coding scheme [4] (H.264) BD-BR	Chen et al.'s intra coding scheme (HEVC) BD-BR	Naive intra coding scheme (HEVC) BD-BR
Boat	20.38–49.05	−44.2	−43.6	−31.7	−7.0	−24.3
Island	25.74–51.01	−43.8	−42.6	−37.5	−5.9	−26.1
Lighthouse	21.58–48.05	−49.7	−48.7	−39.9	−4.7	−23.1
Nature	19.31–48.07	−39.2	−38.9	−32.0	−11.7	−15.5
Average	BD-BR	−44.2	−43.4	−35.3	−7.3	−22.2

Table 3
BD-PSNR (in dB) of the proposed scheme over each compared scheme under other nine non-Bayer CFAs.

CFA type	Video sequence	Bitrate range	Yang et al.'s intra coding scheme [21] (H.264) BD-PSNR	Yang et al.'s intra coding scheme (HEVC) BD-PSNR	Naive intra coding scheme (HEVC) BD-PSNR
Lukac and Plataniotis CFA	Boat	126.4–20055.7	9.61	7.21	6.60
	Island	45.1–15295.7	6.37	3.95	3.71
	Lighthouse	223.6–18879.8	5.81	3.64	4.22
	Nature	125.6–23342.5	10.67	8.78	4.40
Yamanaka CFA	Boat	124.1–19987.7	9.62	7.24	6.71
	Island	45.7–15233.3	6.33	3.87	3.67
	Lighthouse	218.4–18800.8	6.53	3.92	4.25
	Nature	126.1–23379.2	10.69	8.85	4.52
Diagonal stripe CFA	Boat	157.7–20373.7	9.10	7.95	6.09
	Island	49.4–15442.9	6.56	4.33	2.70
	Lighthouse	239.7–19402.0	6.94	4.52	4.21
	Nature	130.4–23443.7	12.20	10.12	4.27
Vertical stripe CFA	Boat	128.7–19826.3	10.94	9.14	3.49
	Island	48.4–15104.8	8.39	5.72	1.97
	Lighthouse	208.5–17967.4	9.81	7.35	1.76
	Nature	141.1–23217.5	12.69	11.07	2.02
Modified Bayer CFA	Boat	117.7–19974.7	10.55	8.48	6.05
	Island	45.2–15235.1	6.90	4.50	3.08
	Lighthouse	213.9–19029.2	6.22	4.05	3.70
	Nature	124.6–23337.6	11.86	10.19	3.72
HVS-based CFA	Boat	98.6–20370.0	11.67	9.39	7.86
	Island	44.5–15429.2	7.83	5.54	5.40
	Lighthouse	152.7–19591.4	8.41	6.16	5.62
	Nature	121.4–23507.8	12.62	10.98	4.25
Type I Pseudo-random CFA	Boat	101.8–20054.8	9.95	7.35	6.72
	Island	45.0–15293.2	6.48	4.00	4.62
	Lighthouse	184.1–19067.6	6.13	3.76	5.09
	Nature	126.6–23419.7	10.93	9.05	4.55
Type II Pseudo-random CFA	Boat	97.9–20335.2	12.61	10.01	7.65
	Island	44.7–15395.9	8.46	6.18	5.36
	Lighthouse	156.6–19709.6	8.93	7.48	5.64
	Nature	122.3–23483.3	13.38	11.70	4.34
Type III Pseudo-random CFA	Boat	103.0–20165.3	10.46	7.94	6.46
	Island	45.4–15431.7	6.69	4.35	4.67
	Lighthouse	162.1–19357.3	6.55	4.36	5.28
	Nature	124.1–23451.9	11.54	9.66	4.03
Average	BD-PSNR		9.18	7.02	4.69

for the lowest three QP values due to the overflowing problems of compression buffer. In general, PSNR increases as bitrate increases for most intra coding schemes. However, in Fig. 10, the PSNRs for intra coding schemes by Chen et al. [4] in both H.264/AVC and HEVC saturate for high values of bitrate since the quality degradation caused by color domain transformation cannot be compensated by the prediction residuals.

For mosaic video sequences with non-Bayer CFA structures, similar results are observed in Figs. 11–19, where the PSNRs for intra coding schemes by Yang et al. [21] in both H.264/AVC and HEVC do not increase significantly for high values of bitrate due to the quality degradation from color domain transformation.

The values of the BD-PSNR and BD-BR for the Bayer CFA and non-Bayer CFA structures are given in Tables 1–4, respectively. Empirical results, in general, show that the proposed intra coding scheme is better than the compared intra coding schemes in terms of BD-PSNR and BD-BR. The improvement over the intra coding schemes in H.264/AVC is even more significant. Results in Tables

Table 4
BD-BR (in %) of the proposed scheme over each compared scheme under other nine non-Bayer CFAs.

CFA type sequence	Video range	PSNR range	Yang et al.'s intra coding scheme [21] (H.264) BD-BR	Yang et al.'s intra coding scheme (HEVC) BD-BR	Naive intra coding scheme (HEVC) BD-BR
Lukac and Plataniotis CFA	Boat	20.37–48.10	−34.4	−7.8	−25.7
	Island	25.75–51.00	−37.0	−6.2	−25.7
	Lighthouse	21.60–48.02	−38.2	−4.0	−24.8
	Nature	19.30–47.10	−32.0	−12.7	−15.0
Yamanaka CFA	Boat	20.39–48.03	−34.7	−9.5	−27.9
	Island	25.76–50.09	−37.3	−3.6	−28.3
	Lighthouse	21.57–45.05	−40.9	−5.4	−30.8
	Nature	19.37–47.06	−37.6	−14.7	−17.6
Diagonal stripe CFA	Boat	20.44–42.07	−39.0	−8.8	−28.4
	Island	25.74–46.09	−43.6	−6.0	−31.0
	Lighthouse	21.62–42.07	−39.6	−1.1	−31.4
	Nature	19.34–40.05	−39.9	−17.3	−18.6
Vertical stripe CFA	Boat	20.56–39.07	−53.7	−31.8	−12.0
	Island	25.67–44.00	−57.7	−33.3	−16.0
	Lighthouse	21.69–38.08	−68.6	−43.3	−12.7
	Nature	19.42–38.06	−50.3	−33.4	−7.7
Modified Bayer CFA	Boat	20.39–43.02	−39.8	−9.2	−26.8
	Island	25.74–47.01	−44.4	−7.4	−29.0
	Lighthouse	21.59–44.01	−39.0	−3.7	−29.0
	Nature	19.36–40.04	−39.7	−19.0	−18.8
HVS-based CFA	Boat	20.38–35.06	−63.2	−6.7	−50.7
	Island	25.72–41.04	−49.6	−6.0	−51.3
	Lighthouse	21.52–35.05	−68.2	0.4	−54.7
	Nature	19.29–34.08	−58.6	−12.9	−31.9
Type I Pseudo-random CFA	Boat	20.37–47.05	−31.2	−4.6	−34.9
	Island	25.75–49.08	−35.2	−1.7	−37.1
	Lighthouse	21.56–46.08	−36.7	−1.0	−36.5
	Nature	19.29–46.02	−37.2	−13.4	−20.2
Type II Pseudo-random CFA	Boat	20.36–31.06	−100.0	−3.6	−57.6
	Island	25.70–38.02	−60.2	5.1	−54.7
	Lighthouse	21.34–31.09	−100.0	2.1	−61.1
	Nature	19.32–30.05	−100.0	−16.8	−39.1
Type III Pseudo-random CFA	Boat	20.36–43.06	−35.6	−10.0	−35.3
	Island	25.73–47.05	−42.5	−4.7	−40.3
	Lighthouse	21.55–42.05	−39.6	−1.8	−43.4
	Nature	19.33–41.09	−37.8	−16.1	−21.6
Average	BD-BR		−48.4	−10.3	−31.3

1 and 3 show that the average BD-PSNR of the proposed intra coding scheme over each compared intra coding scheme ranges from 4.34 dB to 7.74 dB for the Bayer CFA and from 4.69 dB to 9.18 dB for non-Bayer CFAs, indicating significant improvement in the quality of the reconstructed mosaic video sequences. Results in Tables 2 and 4 show that the average BD-BR of the proposed intra coding scheme over each compared intra coding scheme ranges from −7.3% to −44.2% for the Bayer CFA and from −10.3% to −48.4% for non-Bayer CFAs, indicating significant bitrate reduction of the compressed mosaic video sequences.

4.3. When CFA structure is not available

The CFA structure used in the mosaic video sequence is usually provided by the camera manufacturers or obtained from the raw CFA video sequence stored in TIFF-EP format. When the CFA structure is not available, we need to identify the CFA structure prior to intra coding. In this subsection, we evaluate the performance of the proposed algorithm for identifying the CFA structure when the CFA structure used is unknown.

Four video sequences, each with 10 mosaic CFA structures, are used for evaluating the accuracy of the proposed identifying algorithm. The window size used in the identifying algorithm results in different accuracy and computational cost. Larger window sizes yield better accuracy at larger computational cost. When the window size used in Eq. (4) is less than 5×5, there may not exist pixels with identical color component in the neighboring window and hence Eq. (4) is not applicable. When setting the window size used in Eq. (4) to be greater than 7×7, the proposed identifying algorithm achieves 100% accuracy for the testing video sequences. In practice, the set J of possible CFA structures can be extended to include more than 10 commonly used CFA structures for better accuracy. If the CFA structure delivered by the identifying algorithm is not correct, the color-selection based intra prediction may not yield small residuals since the reference pixels are not correctly demosaiced. Furthermore, demosaicing the reconstructed video sequence is further contaminated when adopting the incorrectly identified CFA structure.

Fig. 20 shows the first image frame of video sequence "Lighthouse" with the Bayer CFA structure and the corresponding reconstructed mosaic image with correct Bayer CFA structure and incorrectly identified CFA structures. Since different CFA structures correspond to different arrangements of RGB color components, adopting incorrect CFA structures may result in different degrees of distortion and hue inconsistency in the reconstructed mosaic image when compared with the original mosaic image.

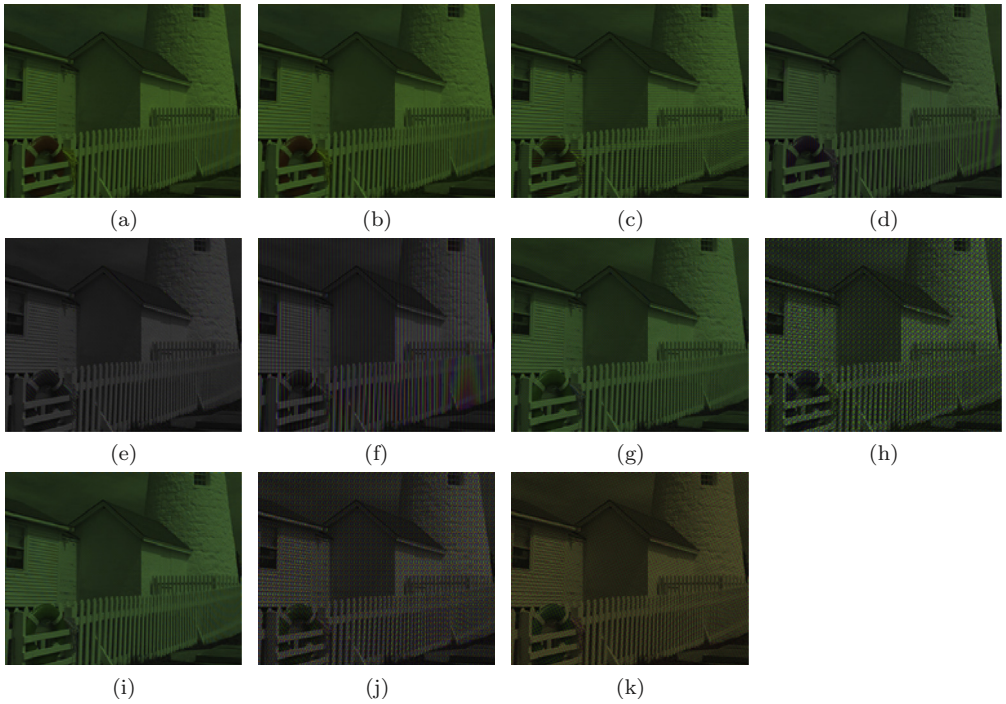

Fig. 20. (a) The first image frame of video sequence "Lighthouse" with the Bayer CFA structure. For QP = 26, the reconstructed mosaic images associated with the proposed intra coding scheme adopting different CFAs: (b) Bayer CFA, (c) Lukac and Plataniotis CFA, (d) Yamanaka CFA, (e) diagonal stripe CFA, (f) vertical stripe CFA, (g) modified Bayer CFA, (h) HVS-based CFA, (i) type I pseudo-random CFA, (j) type II pseudo-random CFA and (k) type III pseudo-random CFA.

5. Conclusions

We present a novel two-stage universal HEVC-based intra coding scheme for compressing mosaic video sequences with arbitrary RGB-CFAs. The proposed scheme first demosaics the neighboring reference pixels and then predicts, according to the mosaic structure, the color value of the target pixel using the color values of the identical components in the reference pixels. The proposed scheme avoids the difficulty in converting irregular CFA structure and the quality degradation caused by color domain transformation. Experimental results demonstrate that the proposed scheme can achieve substantial improvement in both PSNR and bitrate when compared with the existing intra coding schemes. Furthermore, since the proposed intra coding scheme is designed specifically for the RGB-CFAs, it would be interesting to extend the idea to tackle the non-RGB CFAs [11].

Acknowledgments

The work of K.-L. Chung and C.-H. Lin was supported by the National Science Council of ROC under contract NSC101-2221-E-011-139-MY3 and NSC99-2221-E-011-078-MY3. The work of W.-N. Yang was supported by the National Science Council of ROC under contracts NSC101-2218-E-011-001 and NSC101-2218-E-011-005. The work of Y.-H. Huang was supported by the National Science Council of ROC under contract NSC101-2221-E-228-010.

References

[1] B.E. Bayer, Color imaging array, US Patent #3971065, 1976.
[2] G. Bjontegaard, Calculation of average PSNR differences between RD curves, VECG-M33, ITU-T VECG meeting, Austin, TX, 2001, pp. 2–4.
[3] B. Bross, W.J. Han, J.R. Ohm, G.J. Sullivan, T. Wiegand, JCTVC-F803:WD4: working draft 4 of high-efficiency video coding, JCTVC of ITU-T SG16 WP3 and ISO/IEC JTC1/SC29/WG11, 2011.
[4] H. Chen, M. Sun, E. Steinbach, Compression of Bayer-pattern video sequences using adjusted chroma subsampling, IEEE Transactions on Circuits and Systems for Video Technology 19 (12) (2009) 1891–1896.
[5] K.H. Chung, Y.H. Chan, Color demosaicing using variance of color differences, IEEE Transactions on Image Processing 15 (10) (2006) 2944–2955.
[6] K.L. Chung, W.J. Yang, W.M. Yan, C.C. Wang, Demosaicing of color filter array captured images using gradient edge detection mask and adaptive heterogeneity-projection, IEEE Transactions on Image Processing 17 (12) (2008) 2356–2367.
[7] C. Doutre, P. Nasiopoulos, K.N. Plataniotis, H.264-based compression of Bayer pattern video sequences, IEEE Transactions on Circuits and Systems for Video Technology 18 (6) (2008) 725–734.
[8] C. Doutre, P. Nasiopoulos, Modified H.264 intra prediction for compression of video and images captured with a color filter array, in: Proc. of IEEE Int. Conf. on Image Processing (ICIP 2009), 2009, pp. 3401–3404.
[9] F. Gastaldi, C.C. Koh, M. Carli, A. Neri, S.K. Mitra, Compression of videos captured via Bayer patterned color filter arrays, in: Proc. of 13th European Signal Processing Conf., 2005, pp. 1–4.
[10] B. Gunturk, Y. Altunbasak, R. Mersereau, Color plane interpolation using alternating projections, IEEE Transactions on Image Processing 11 (9) (2002) 997–1013.
[11] K. Hirakawa, P.J. Wolfe, Spatio-spectral color filter array design for optimal image recovery, IEEE Transactions on Image Processing 17 (10) (2008) 1876–1890.
[12] C.C. Koh, J. Mukherjee, S.K. Mitra, New efficient methods of image compression in digital cameras with color filter array, IEEE Transactions on Consumer Electronics 49 (4) (2003) 1448–1456.
[13] J.S.J. Li, S. Randhawa, Color filter array demosaicing using high-order interpolation techniques with a weighted median filter for sharp color edge preservation, IEEE Transactions on Image Processing 18 (9) (2009) 1946–1957.
[14] W. Lu, Y.P. Tang, Color filter array demosaicing: new method and performance measures, IEEE Transactions on Image Processing 12 (10) (2003) 1194–1210.
[15] R. Lukac, K.N. Plataniotis, Universal demosaicing for imaging pipelines with an RGB color filter array, Pattern Recognition 38 (11) (2005) 2208–2212.
[16] R. Lukac, K.N. Plataniotis, Color filter arrays: design and performance analysis, IEEE Transactions on Consumer Electronics 51 (4) (2005) 1260–1267.
[17] R. Lukac, K.N. Plataniotis, D. Hatzinakos, M. Aleksic, A new CFA interpolation framework, Signal Processing 86 (7) (2006) 1559–1579.
[18] R. Lukac, Single-Sensor Imaging: Methods and Applications for Digital Cameras, CRC Press/ Taylor and Francis, Boca Raton, FL, 2008.
[19] D. Menon, G. Calvagno, Regularization approaches to demosaicing, IEEE Transactions on Image Processing 18 (10) (2009) 2209–2220.
[20] S.C. Pei, I.K. Tam, Effective color interpolation in CCD color filter arrays using signal correlation, IEEE Transactions on Circuits and Systems for Video Technology 13 (6) (2003) 503–513.
[21] W.J. Yang, K.L. Chung, W.N. Yang, L.C. Lin, Universal chroma subsampling strategy for compressing mosaic video sequences with arbitrary RGB color filter arrays in H.264/AVC, IEEE Transactions on Circuits and Systems for Video Technology 23 (4) (2013) 591–606.

[22] L. Zhang, X. Wu, Color demosaicing via directional linear minimum mean square-error estimation, IEEE Transactions on Image Processing 14 (12) (2005) 2167–2178.
[23] L. Zhang, W. Dong, X. Wu, G. Shi, Spatial-temporal color video reconstruction from noisy CFA sequence, IEEE Transactions on Circuits and Systems for Video Technology 20 (6) (2010) 838–847.
[24] L. Zhang, X. Wu, A. Buades, X. Li, Color demosaicing by local directional interpolation and non-local adaptive thresholding, Journal of Electronic Imaging 20 (2) (2011) 023016.
[25] Draft ITU-T recommendation and final draft international standard of joint video specification (ITU-T Rec. H.264/ISO/IEC 14496–10 AVC), JVT of ISO/IEC and ITU-T, 2003.
[26] Generic coding of moving pictures and associated audio (MPEG-2), ISO/IEC 13818, 1995.
[27] Quality of RGB-YUV-RGB conversion, Available: <http://discoverybiz.net/enu0/faq/faq_YUVbyBreeze_test_00.html> (Online).
[28] Available: <http://140.118.175.164/YHChiu/paper/UniversalIntraCoding/> (Online).